Romanian Reports in Physics **73**, 408 (2021)

THEORETICAL STUDY OF THE BEHAVIOR OF A DBR LASER SUBJECT TO EXTERNAL OPTICAL FEEDBACK

VASILE TRONCIU[1,*], NILS WERNER[2], HANS WENZEL[2], HANS JÜRGEN WÜNSCHE[2]

[1]Department of Physics, Technical University of Moldova, Chisinau MD-2004, Republic of Moldova
[2]Ferdinand-Braun-Institut gGmbH, Leibniz-Institut für Höchstfrequenztechnik, Gustav-Kirchhoff-Str. 4, 12489 Berlin, Germany
*Corresponding author, Email: *vasile.tronciu@fiz.utm.md*

Received August 26, 2021

Abstract. We report results of the theoretical study of the dynamic properties of distributed Bragg reflector (DBR) lasers subject to an external optical feedback provided by a long-distance mirror. We adapt the Lang-Kobayashi (LK) model to the considered device. The adapted parameters Henry factor, photon life time, feedback strength, and modal group index entering the LK model depend strongly on the lasing wavelength of the solitary laser. The stationary states computed by the full and adapted LK models show good agreement. We consider the external reflectivity and phase and the solitary laser wavelength as a bifurcation parameters. Thus, we investigate the impact of these parameters on the stability of the stationary states.

Key words: DBR lasers, optical feedback, bifurcation diagram, detuning.

1. INTRODUCTION

During recent years high-power distributed Bragg reflector (DBR) lasers have received more and more interest since they enable single longitudinal mode operation with a small spectral linewidth. Such devices are requested by a number of emerging applications such as second harmonic generation, spectroscopy, quantum metrology, and optical communication [1–3]. However, within complex experimental setups unwanted optical feedback can appear either from interconnections or from external mirrors. It is well known that an external feedback affects the laser emission including coherence collapse, emission frequency shift, changes in the spectral line width etc. [4–6]. Recently, the impact of weak feedback on high-power DBR tapered and distributed feedback (DFB) lasers was reported in [7] and [8]. The measured data for the induced frequency shift in dependence on the external cavity length were analyzed on the basis of the classical Lang–Kobayashi (LK) equations [9] strictly valid only for Fabry-Perot (FP) lasers. The influence of strong optical feedback on the emission behavior of DBR ridge waveguide (RW) lasers emitting at 1120 nm having different cavity lengths and facet reflectivities was investigated in [10].

In this paper we derive the modified parameters entering the LK equations valid for DBR lasers having a frequency-dependent Bragg reflector. This allows an inves-

tigation of the influence of internal parameters such as the sectional lengths and the detuning with respect to the Bragg wavelength on the behavior of the DBR laser subject to weak external feedback. The configuration considered is shown in Fig. 1a. The emission from the facet of the active section of the DBR laser at $z = 0$ is injected to a simple mirror with constant power reflectivity R and phase φ in a distance L from the facet and fed back from there. Figure 1b shows the spectrum of the intensity reflectivity of the Bragg grating for the set of parameters shown in Table 1.

Table 1

Parameters of the standard configuration

Symbol	Description	Unit	Value
	solitary laser:		
λ_{l}	laser wavelength	m	$1.12 \cdot 10^{-6}$
n_{g}	group refractive index		3.6
	DBR section:		
L_κ	length	m	$1 \cdot 10^{-3}$
α_κ	optical waveguide losses	m^{-1}	200
λ_κ	central wavelength	m	$1.12 \cdot 10^{-6}$
κ	coupling coefficient	m^{-1}	$7.5 \cdot 10^{2}$
ϕ_κ	phase of coupling coefficient		0
	facet reflectivity		0
	active section:		
L_a	length	m	$(0.5,\ \mathbf{1},\ 2,\ 3) \cdot 10^{-3}$
β_0	wavevector	m^{-1}	0
Δn_{eff}	index detuning		$-2.1798 \cdot 10^{-4}$
α_a	optical waveguide loss	m^{-1}	200
α_{H}	Henry factor		1.2
R_a	facet reflectivity		0.1
φ_r	phase shift	rad	0
φ_t	phase shift	rad	0
τ_N	effective carrier lifetime	s	$1.67 \cdot 10^{-9}$
	feedback part:		
L	optical length	m	0.6
R	reflectivity		$10^{-6} \ldots 10^{-3}$
φ	round-trip phase shift	rad	$-\pi \ldots \pi$

The paper is structured as follows. In Sec. 2 the theoretical model is described. The dynamical equations of the adjusted LK model for DBR lasers with feedback are derived in Sec. 3. In Sec. 4 the stationary states computed with the LK model

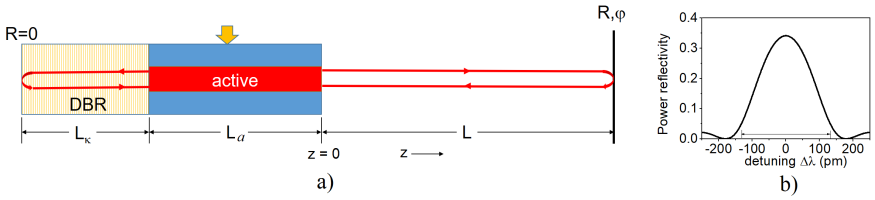

Fig. 1 – (Color online) a) Scheme of the setup, b) power reflection spectrum of the Bragg reflector of the laser.

and the full model are compared. An analysis of the stability of the stationary states is presented in Sec. 5. Finally, summary and conclusions are given in Sec. 6.

2. MODEL AND EQUATIONS

Under continuous wave (CW) operation, the carrier densities as well as the optical power in the DBR laser are constant in time. Within the whole laser, two counter propagating waves of the following form are circulating

$$E(z,t) = \left[E^+(z,t,\omega_s)\mathrm{e}^{-i\beta_0 z} + E^-(z,t,\omega_s)\mathrm{e}^{i\beta_0 z}\right]\mathrm{e}^{i\omega_s t}, \tag{1}$$

where $\beta_0 = n\pi/\Lambda$ with order n and period Λ of the grating in the DBR.

In a stationary state, the laser emits and receives back monochromatic light of frequency ω_s with the respective constant in time amplitudes $E^+(\omega_\mathrm{s}) \equiv E^+(0,t,\omega_\mathrm{s})$ and $E^-(\omega_\mathrm{s}) \equiv E^-(0,t,\omega_\mathrm{s})$, measured at a reference plane $z = 0$ just outside the laser facet. The two amplitudes are related to each other by

$$E^-(\omega_\mathrm{s}) = r_\mathrm{f}(\omega_s)E^+(\omega_\mathrm{s}) \text{ and } E^+(\omega_\mathrm{s}) = r_\mathrm{l}(\omega_\mathrm{s},g_s)E^-(\omega_\mathrm{s}), \tag{2}$$

where $r_\mathrm{f}(\omega_s)$ is the full reflectivity of the whole feedback arm seen from left at $z = 0$. Likewise, $r_\mathrm{l}(\omega_\mathrm{s},g_s)$ denotes the full reflectivity of the DBR laser (active + DBR sections) for light coming from the reference plane at frequency ω_s and gain g_s of the stationary state. Note that our reference plane is located outside of the laser. Nonzero amplitudes require the validity of the round-trip condition

$$r_\mathrm{f}(\omega_s) = q(\omega_s,g_s), \qquad \text{with} \qquad q(\omega_s,g_s) := r_\mathrm{l}^{-1}(\omega_\mathrm{s},g_s), \tag{3}$$

which solution yields ω_s and g_s of the stationary state. Without feedback, q must become zero.

In the next step we construct the reflectivities entering (2). The reflectivity from the right hand side of a grating is [11]

$$r_\kappa = \frac{-i\kappa^+\frac{\sin(\gamma L_\kappa)}{\gamma}}{\cos(\gamma L_\kappa) + i\Delta\beta\frac{\sin(\gamma L_\kappa)}{\gamma}} \quad \text{with} \quad \gamma = \sqrt{(\Delta\beta_\kappa)^2 - \kappa^+\kappa^-}, \tag{4}$$

where L_κ is the length of the grating and

$$\Delta\beta_\kappa(\lambda) = \beta_\kappa(\lambda) - \beta_0, \quad \beta_\kappa = \frac{2\pi}{\lambda} n_\kappa(\lambda) - \frac{i}{2}\alpha_\kappa, \quad \kappa^\pm = \kappa \mathrm{e}^{\mp 2\pi i \varphi_\kappa}. \tag{5}$$

Here κ is the coupling coefficient of the grating, n_κ is the modal index of the internal waveguide, α_κ is the background absorption coefficient of the guided waves in the grating section, and φ_κ is a phase shift depending on the relative position of the grating with respect to the right facet of the DBR. We introduce the so-called Bragg wavelength λ_κ at the maximum of the reflection spectrum of the grating (center of the stop band) where

$$\mathrm{Re}\{\beta_\kappa(\lambda_\kappa)\} = \beta_0 \tag{6}$$

holds. Our DBR is relatively long and has a small κ. Hence, the width of its dominating reflection spectrum (stop band) - where the lasing modes are residing - is small. Within its range we can use the linearization

$$\beta_\kappa(\lambda) = \beta_0 - \frac{i}{2}\alpha_\kappa - \frac{2\pi}{\lambda_\kappa^2} n_\mathrm{g} \Delta\lambda \tag{7}$$

where n_g is the modal group index in both DBR and active sections and $\Delta\lambda = \lambda - \lambda_\kappa$ is the wavelength relative to the Bragg wavelength. For transforming to the LK equations, it is better to use circular frequencies instead of wavelengths. The central frequency is $\omega_\kappa = 2\pi c/\lambda_\kappa$ and the relative frequency is $\Delta\omega = -\omega_\kappa \Delta\lambda/\lambda_\kappa$. With these quantities we have

$$\beta_\kappa(\omega) = \beta_0 - \frac{i}{2}\alpha_\kappa + \frac{\Delta\omega}{v_\mathrm{g}}, \tag{8}$$

where the modal group velocity is $v_g = c/n_g$.

Now we introduce the round-trip propagator of the active section $\mathcal{P}(\omega, g) = r_\kappa(\omega) r_+ \exp[-2i\beta_a(\omega, g) L_a]$ and the reflectivities of the facet at the active section $r_\pm = \sqrt{R_a} e^{-i\varphi_\pm}$ with $\varphi_+ = \pi + \varphi_\mathrm{r}$ and $\varphi_- = -\varphi_\mathrm{r} + 2\varphi_t$ [12, 13]. They agree with the slowly-varying-amplitude reflectivites because we set $z = 0$ at this facet. R_a is the corresponding power reflectivity. The propagation constant of the active section is modeled as

$$\beta_a(\omega, g) = \beta_0 + \frac{2\pi}{\lambda_\kappa}\Delta n_\mathrm{eff} - \frac{i}{2}\alpha_a + (1 + i\alpha_\mathrm{H})\frac{i}{2} g + \frac{\Delta\omega}{v_\mathrm{g}}. \tag{9}$$

The possible index detuning Δn_eff between active and DBR sections may be due to current induced heating of the active section. $\alpha_\mathrm{a,H}$ is the Henry-factor of the active waveguide. g is the modal gain, and α_a is the background absorption in the active section. The right hand side (rhs) of (3) reads then

$$q(\omega, g) = \left(\frac{R_a}{r_-}\right) \frac{1 - \mathcal{P}(\omega, g)}{R_a - \mathcal{P}(\omega, g)}. \tag{10}$$

Without feedback $\mathcal{P}(\omega_l, g_l) = 1$ must hold. Here, the frequency ω_l of the solitary laser is treated as a parameter, which is moved across the stop band of the DBR section. The solution of $|\mathcal{P}(\omega_l, g_l)| = 1$ yields the threshold condition

$$g_l = \alpha_a - \frac{1}{L_a} \ln(|r_\kappa(\omega_l)| \sqrt{R_a}). \tag{11}$$

Lasing at ω_l requires also that $\arg \mathcal{P}(\omega_l, g_l)$ is an integer multiple of 2π. For a given laser, this selects a countable set of frequencies, the longitudinal modes, which have to be determined by iterations. In our case of a given ω_l, this phase condition selects a countable set of different lasers, namely those fulfilling

$$\left[\left(\frac{4\pi}{\lambda_\kappa} \Delta n_{\text{eff}} - \alpha_{\text{H}} g_l + \frac{2\Delta\omega_l}{v_g} + \frac{2\pi}{\Lambda} \right) L_a - \arg(r_\kappa(\omega_l) r_+) \right] \mod 2\pi = 0. \tag{12}$$

So, by setting ω_l, we can determine the corresponding threshold gain g_l and a related index detuning Δn_{eff} analytically with no iterations.

The reflectivity of the feedback part has the simple form

$$r_f(\omega) = \sqrt{R} \mathrm{e}^{-i(\varphi + \omega\tau)}. \tag{13}$$

The φ contains a possible phase shift of the external mirror and also all phase shifts due to the coupling optics within the feedback path. Accordingly does the delay τ and the reflectivity R of the feedback arm. In the next Section we analyze the stability of CW operation in the framework of the LK equations, which are restricted to weak feedback. In this case, $q(\omega_s, g_s)$ remains close to its zero at $\omega_\text{s} = \omega_\text{l}$, $g_\text{s} = g_\text{l}$ and can be linearized. Before doing that, it is useful to insert the derived expressions and to multiply the round-trip condition (3) with $r_\text{-}/R_a = e^{i \arg(r_\text{-})}/\sqrt{R_a}$, yielding

$$\sqrt{R/R_a} \mathrm{e}^{-i(\varphi + \omega_s \tau - \arg(r_\text{-}))} = \tilde{q}(\omega_s, g_s), \tag{14}$$

$$\text{with } \tilde{q}(\omega_s, g_s) = \frac{1 - \mathcal{P}(\omega_s, g_s)}{R_a - \mathcal{P}(\omega_s, g_s)} \tag{15}$$

Now the phase of $r_\text{-}$ belongs to the feedback arm. Since $\tilde{q}$ vanishes at the chosen longitudinal mode, the linearization is

$$\tilde{q}(\omega, g) = \partial_\omega \tilde{q} \cdot (\omega - \omega_l) + \partial_g \tilde{q} \cdot (g - g_l), \tag{16}$$

where ∂_ω and ∂_g means the partial derivative. Inserting (16) into the round-trip condition (14) and dividing by $-i\partial_\omega \tilde{q}$ yields

$$i(\omega_\text{s} - \omega_\text{l}) - \frac{\tilde{v}_\text{g}}{2}(1 + i\tilde{\alpha}_\text{H})(g_\text{s} - g_\text{l}) = \eta e^{-i\phi} Q(\omega_s), \tag{17}$$

$$\tilde{v}_g = 2\text{Im}(\partial_g \tilde{q}/\partial_\omega \tilde{q}), \quad \tilde{\alpha}_\text{H} = -\frac{\text{Re}(\partial_g \tilde{q}/\partial_\omega \tilde{q})}{\text{Im}(\partial_g \tilde{q}/\partial_\omega \tilde{q})}, \tag{18}$$

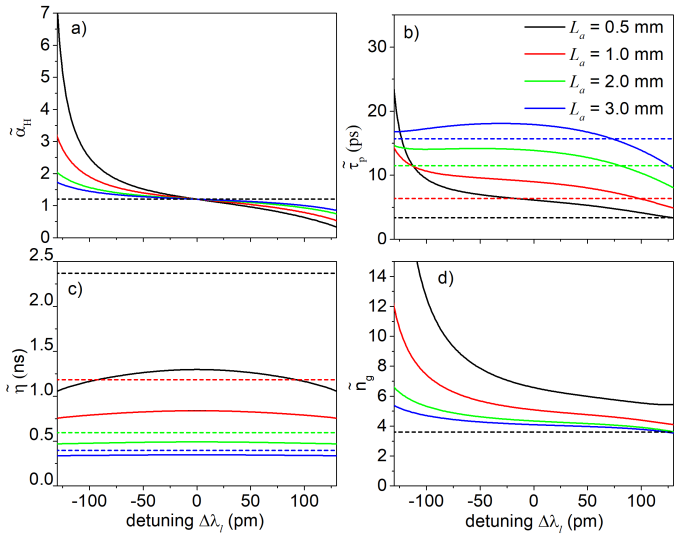

Fig. 2 – (Color online) The dependence of scaled parameters entering the LK equations on the detuning of the mode of the solitary laser: a) Henry factor $\tilde{\alpha}_{\rm H}$, b) photon life time $\tilde{\tau}_{\rm p}$, c) feedback strength $\tilde{\eta}$, and d) group index $\tilde{n}_{\rm g}$. Solid lines: DBR laser, dotted lines: FP laser (see text).

and the rescaled feedback parameters

$$\tilde{\eta} = \frac{\sqrt{R/R_a}}{|\partial_{\omega_{\rm s}}\tilde{q}|}, \tag{19}$$

$$\phi = \varphi + \arg(\partial_{\omega_{\rm s}}\tilde{q}) - \frac{\pi}{2} - \arg(r_-), \tag{20}$$

$$Q(\omega_s) = e^{-i\omega_{\rm s}\tau}, \tau = 2L/c. \tag{21}$$

The rescaled photon life time is $\tilde{\tau}_{\rm p} = (\tilde{v}_{\rm g} g_{\rm l})^{-1}$. The rescaled parameters distinguished with a tilde depend on the relative wavelength $\Delta\lambda_l = \lambda_l - \lambda_\kappa$, the so called detuning of the solitary laser wavelength. On the other hand, these parameters also depend on the structural parameters such as coupling coefficient, length of DBR, active sections etc.

Let us consider what is predicted to happen, when we vary the solitary mode detuning and calculate $\tilde{\alpha}_H$, $\tilde{\tau}_p$, $\tilde{\eta}$, and $\tilde{n}_{\rm g} = c/\tilde{v}_{\rm g}$. The results are shown in Fig. 2 for different lengths L_a of the active section. The dotted lines are the results for a FP laser where the DBR is replaced by a mirror a $z = -L_a$. The mirror has a frequency-independent reflectivity which value is given by the peak reflectivity of the Bragg reflector of 0.34 (see Fig. 1b). The shorter the length of the active section, the larger the deviation to the dotted lines and the larger is the variation across the stop band. A large variation can be observed for the rescaled Henry α-factor $\tilde{\alpha}_H$. It is well-known that a higher Henry factor results in a more unstable behavior. It can

be clearly seen, that for positive detuning where $\tilde{\alpha}_H$ is reduced below the material value, the laser should be more immune to feedback, whereas for negative detuning strong instabilities are to be expected.

3. THE DYNAMICAL EQUATIONS

It is well known that the stationary state is locally stable if the system returns to it upon all sufficiently small deviations. When changing a parameter, this decay can become slower and even turn into the existence of arbitrarily small deviations growing with time, which necessarily leads to a self-sustaining dynamics or causes a transition to another stationary state that is stable. The bifurcation analysis of stationary states requires dynamical equations for the temporal evolution in their neighborhood. Dynamical equations for the slowly varying amplitudes $E^+(t)$ and $E^-(t)$ are generally obtained by Fourier transforming the feedback equations (2) into time domain, treating the gain adiabatically as a parameter. The adiabatic approximation for the gain is uncritical because the build-up time of the DBR reflectivity of only a few ps is much smaller than the characteristic time for gain changes. Here and in the following we use the same letter for a function in time domain and in frequency domain because it is always clear from context what is meant. Additionally we denote $E^+(t)$ simply as $E(t)$.

Before Fourier transforming, we make the following approximations for the two reflection coefficients. First, $q = r_l^{-1}$ is linearized at its zero in the sense of the weak-feedback approximation introduced in the last Section. The Fourier transform of $i\omega E^+(\omega)$ yields the term $\dot{E}(t)$ in (22) below. The other terms come from the substitutions $\tilde{v}_g(g(t)-g_l)/2 = N(t)/\tilde{\tau}_p$ and $E^-(t) = \sqrt{R}e^{-i\varphi}E(t-\tau)$ with the dimensionless inversion $N(t) = \frac{g(t)-g_l}{2g_l}$, and the photon life time $\tilde{\tau}_\mathrm{p} = (\tilde{v}_\mathrm{g} g_\mathrm{l})^{-1}$. Adding furthermore the standard rate equation for the dimensionless inversion $N(t)$ with the unsaturated inversion $N_0 = 0.5(I - I_\mathrm{th})/(I_\mathrm{th} - I_\mathrm{tr})$ (I_th threshold current, I_tr transparency current) and the carrier life time τ_N and scaling the amplitudes appropriately, the full set of dynamical equation is

$$\dot{E}(t) = \left[i\omega_\mathrm{l} + (1 + i\tilde{\alpha}_\mathrm{H}) \frac{N(t)}{\tilde{\tau}_\mathrm{p}} \right] E(t) + \eta e^{-i\phi} E(t-\tau) \tag{22}$$

$$\dot{N}(t) = \frac{1}{\tau_\mathrm{N}} \left[N_0 - N(t) - (1 + 2N(t))|E(t)|^2 \right]. \tag{23}$$

All notations and transformations are the same as in [14], with replacing $\alpha_\mathrm{H}, v_g, \tau_p$, and η by the rescaled versions (18)-(21).

This system represents the well known standard LK equations [9] for a semiconductor laser subject to delayed optical feedback. They have been widely studied

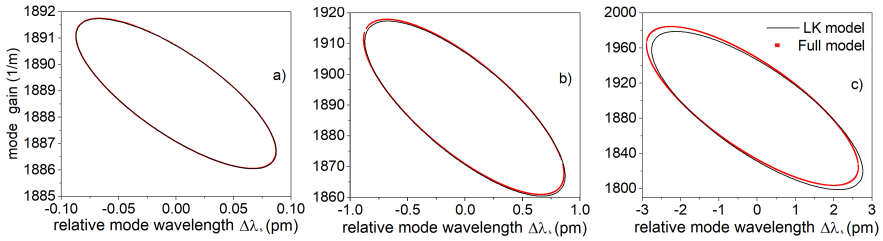

Fig. 3 – (Color online) Stationary gain *versus* relative stationary wavelength of the LK (black line) and full (red dots) models for different feedback reflectivities. a) $R = 10^{-6}$, b) $R = 10^{-4}$, c) $R = 10^{-3}$. Length of active section $L_a = 1.0$ mm. Other parameters are as in Table 1.

and one could think there is nothing new because it is easy just to take over these results to the present case. However, the situation is a bit more complicated. We want to study the stability of solitary laser modes in dependence on their spectral position $\Delta\lambda_l = \lambda_l - \lambda_\kappa$ relative to the center of the DBR stop band for fixed other parameters. Therefore, we redo the bifurcation analysis for this parameter path. Since the LK equations are delay-differential equations (DDE), we apply the software DDE-biftool [15] to these purposes. It allows to compute branches of stationary solutions and to follow their bifurcations in the parameter space. Furthermore, the periodic solutions can be continued starting from previously computed Hopf bifurcations. The mathematical background, in particular in view of the rotational symmetry of laser DDEs, is described in detail in Refs. [4, 5].

4. VALIDATION OF THE MODEL

In what follows, we consider the stationary lasing states called external cavity modes (ECMs), which are either solutions of (3) (full model) or rotating wave solutions of the LK model (22)-(23). It is well known, that for the weak optical feedback the ECMs are located on ellipses in the plane $g_s - \Delta\lambda_s$ of mode gain and relative mode wavelength. Here we compare the ECMs computed by employing the LK model with rescaled parameters and the full model. Figure 3 shows the ellipses for different feedback reflectivities. For an external reflectivity of $R = 10^{-6}$, there is an excellent agreement between both models and the ellipses overlap very well. An increase of the external reflectivity to $R = 10^{-4}$ and further to $R = 10^{-3}$ results in rising deviations between the models, although the agreement is still reasonable.

Figure 4 shows the dependence of the stationary gain and the relative stationary wavelength $\Delta\lambda_s = \lambda_s - \lambda_\kappa$ on the detuning $\Delta\lambda_l$ and the external phase φ for $R = 10^{-4}$. For both dependencies, the phenomena of bistability and multistability can be clearly seen. The agreement between both models is again very good. Thus, we conclude that for an external reflectivity of $R < 10^{-3}$ we can successfully apply the

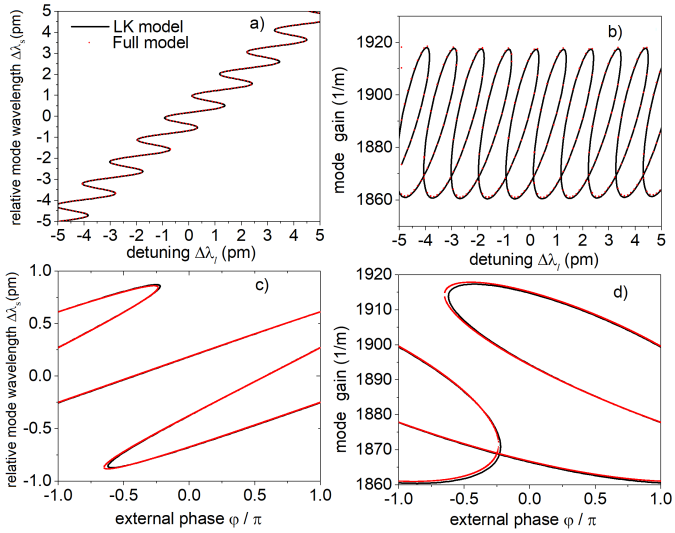

Fig. 4 – (Color online) Relative stationary wavelength a), c) and stationary gain b), d) *versus* the relative wavelength of the solitary laser a), b) and the external phase c), d), respectively, for the LK (black line) and full (red dots) models. The length of active section $L_a = 1.0$ mm and the external reflectivity $R = 10^{-4}$. The other parameters are the same as in Fig. 3.

LK model to our setup shown in Fig. 1.

5. STABILITY ANALYSIS OF STATIONARY STATES

Here we use *DDE-biftool* [15] to analyze the stability of the ECMs based on a continuation method. Figure 5 shows the ellipses for $R = 10^{-4}$ for different lengths L_a of the active section, resulting in different values of g_l and hence different sizes of the ellipses. The gray lines show a saddle-node (SN) bifurcation for any values of the external reflectivity R. The intersection points between this line and the ellipses shown by gray bullets represent SN bifurcations for $R = 10^{-4}$, separating ECMs called 'anti-modes' (red lines).

DDE-biftool allows to find Hopf bifurations marked by a black square in Fig. 5 separating stable (green line) and unstable (blue line) ECMs. It can be clearly seen that the instability region (blue line) decreases with increasing L_a and disappears for $L_a = 3$ mm.

Figure 6 shows Hopf lines separating stable regions from unstable ones in the plane of two device parameters, namely the external reflectivity R and the external phase φ, for the same lengths as in 5. Note, that the other Hopf lines obtained by a repetition with a period of 2π are not shown. This figure confirms the results of previous findings [16] and also those of Ref. [17] where a semi-analytical model

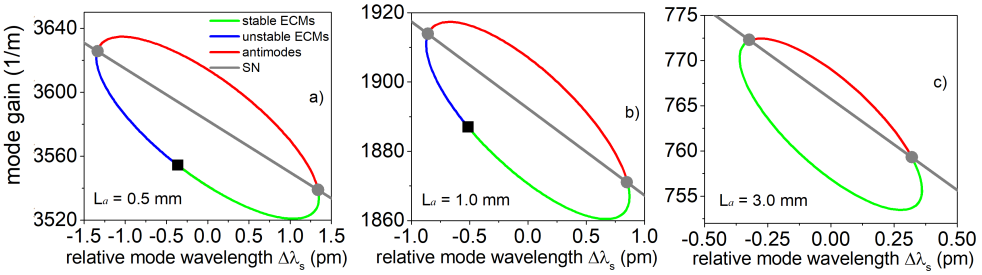

Fig. 5 – (Color online) Stationary gain *versus* relative stationary wavelength for external reflectivity of $R = 10^{-4}$, detuning $\Delta\lambda_l = 0$ and different values of the length of the active section. a) $I_{\rm tr} = 0.006523$ A, $I_{\rm th} = 0.019$ A, $I = 0.04379$ A, b) $I_{\rm tr} = 0.013$ A, $I_{\rm th} = 0.0262$ A, $I = 0.0524$ A, c) $I_{\rm tr} = 0.03914$ A, $I_{\rm th} = 0.05511$ A, $I = 0.0868$ A. Solid green line–stable stationary states. Blue line–unstable stationary states. Square–Hopf bifurcation. Gray bullet–saddle node bifurcation (SN) for $R = 10^{-4}$. Gray line–saddle node bifurcation for any reflectivity.

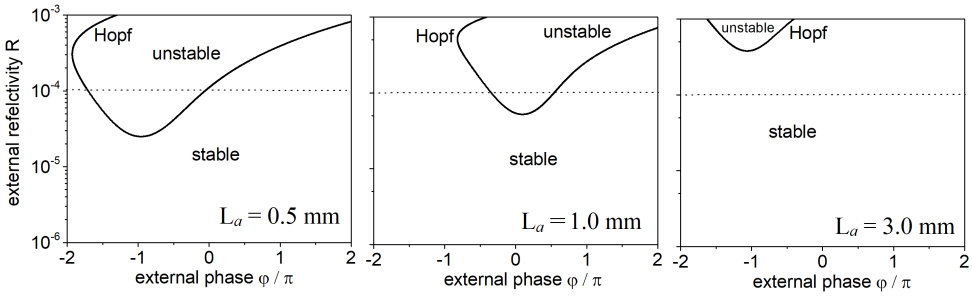

Fig. 6 – Hopf bifurcation in the plane of two parameters (external reflectivity R - external phase φ) for different lengths of the active section. The other parameters are the same as in Fig. 5.

was used. The minimum external reflectivity leading to a Hopf bifurcation for some external phase rises with increasing L_a. A laser with a long active section is more prone to feedback than that with a short one.

Figure 7 shows the dependence of the relative stationary mode wavelength $\Delta\lambda_s$ on the detuning $\Delta\lambda_l$ of the solitary mode wavelength for $L_a = 1$ mm. The right column in Fig. 7 contains magnified views of areas A, B, and C, respectively. For positive detuning (area A) there are only SM bifurcations but no Hopf bifurcation and hence only antimodes but no unstable ECMs exist. However, one can observe a bistable behavior. The analysis of area B (zero detuning) shows that the stable region (green line) is terminated by a Hopf bifurcation, and a region with instabilities appears. Moreover, for negative detuning (area C) the region of instabilities becomes wider, and multistability appears. Thus, we conclude that the detuning of the solitary mode wavelength influences drastically the stability of the stationary states. The root cause is the dependence of the scaled parameters entering the LK equations, in

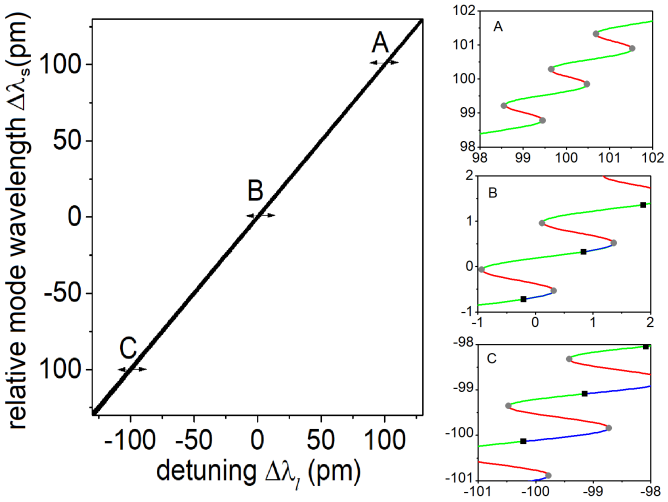

Fig. 7 – (Color online) Relative stationary wavelength $\Delta\lambda_s$ *versus* solitary detuning $\Delta\lambda_l$ for $L_a = 1$ mm, $R = 10^{-4}$, and $\varphi = 0$. Right column: The areas A, B, and C zoomed. The symbols and line colors are the same as in Fig. 5.

particular the Henry factor, on $\Delta\lambda_l$ as shown in Fig. 2.

6. CONCLUSION

We have carried out theoretical investigations of the behavior of a distributed Bragg laser (DBR) laser subject to external feedback. The case of a long feedback branch is considered. A full model and an adapted Lang-Kobayashi model have been used to compute the stationary states. A good agreement for external reflectivities smaller than 10^{-3} has been obtained. The adapted Henry factor, photon life time, feedback strength, and modal group index entering the LK model strongly depend on the detuning between the lasing wavelength and the Bragg wavelength.

We have performed a bifurcation analysis considering the stability of the stationary states, *i.e.* the external cavity modes. The stability is lost by Hopf bifurcations. We have found that DBR lasers with short active sections are characterized by wider unstable regions compared to those of long ones. We ascribe the existence of a wide region of instability for negative detuning to the high values of the adapted Henry factor characteristic for this region. A positive detuning implies a reduction of the unstable region (low alpha factor), even a disappearance for higher positive detuning.

We believe that our work provides a good basis for future studies and, in particular, provides some hints for more detailed experimental investigations of DBR

lasers and their applications as a stable single mode source of light.

Acknowledgements. This work was partly supported by the National Agency for Research and Development of Moldova within the project 20.80009.5007.08 "Study of optoelectronic structures and thermoelectric devices with high efficiency".

REFERENCES

1. J. Hofmann, A. Sahm, W. John, F. Bugge, and K. Paschke, Optics and Laser Technology **83**, 55 (2016).
2. N. Herschbach, P. Tol, W. Vassen, W. Hogervorst, G. Woestenenk, J. Thomsen, P. van der Straten, and A. Niehaus, Phys. Rev. Lett. **84**, 1874 (2000).
3. Z. Sodnik, B. Furch, and H. Lutz, IEEE J. Sel. Top. Quantum Electron. **16**, 1051 (2010).
4. S. M. V. Lunel and B. Krauskopf, AIP Conference Proceedings, vol. 548, B. Krauskopf and D. Lenstra Eds., American Institute of Physics Publishing, Melville (New York), pp. 66–86 (2000).
5. B. Krauskopf, in *Unlocking Dynamical Diversity: Optical Feedback Effects on Semiconductor Lasers*, D. M. Kane and K. A. Shore Eds., Wiley, 147–183 (2005).
6. V. Tronciu, R. Arar, and H. Wenzel, Romanian Reports in Physics **72**, 411 (2020).
7. M. Christensen, C. Zink, M. Tahir Jamal, A. K. Hansen, O. B. Jensen, and B. Sumpf. Journal of the Optical Society of America B **38**(3), 885 (2021).
8. C. Zink *et al.*, Proc. of SPIE **10939**, 109391J-1 (2019).
9. R. Lang and K. Kobayashi, IEEE J. Quantum Electron. **16**(3), 347 (1980).
10. N. Werner, J. Wegemund, D. Feise, K. Paschke, and G. Tränkle, Applied Optics **59**(28), 8653 (2020).
11. H. Wenzel, R. Güther, A. Shams-Zadeh-Amiri, and P. Bienstman, IEEE J. Quantum Electron. **42**(1), 64 (2005).
12. L. A. Coldren *et al.*, *Diode Lasers and Photonic Integrated Circuits*, John Wiley & Sons, Inc., Hoboken, New Jersey (2012).
13. M. A. Dupertuis, B. Acklin, and M. Proctor, J. Opt. Soc. Am. A **11**(3), 1167 (1994).
14. V. Tronciu, H. Wenzel, and H. J. Wünsche, IEEE J. Quantum Electron. **53**(1), 2200109 (2017).
15. J. Sieber, K. Engelborghs, T. Luzyanina, G. Samaey, and D. Roose, DDE-BIFTOOL v.3.1 Manual - Bifurcation analysis of delay differential equations.
16. G. Morthier, IEEE Photonics Journal **13**(4), 1500205 (2021).
17. V. Tronciu, N. Werner, H. Wenzel, and H. J. Wünsche, IEEE J. Quantum Electron. **57**(5), 2100107 (2021).